Development 109, 11–16 (1990)
Printed in Great Britain © The Company of Biologists Limited 1990

Curvature and spiral geometry in aggregation patterns of *Dictyostelium discoideum*

P. FOERSTER, S. C. MÜLLER and B. HESS

Max-Planck-Institut für Ernährungsphysiologie, Rheinlanddamm 201, D-4600 Dortmund 1, FRG

Summary

Aggregation patterns of the slime mould *Dictyostelium discoideum* were recorded using dark-field equipment combined with video techniques. Computerized image processing allowed the analysis of wave collision structures, expanding concentric circles and rotating spirals in terms of wave velocity and front geometry, as previously done in the Belousov-Zhabotinskii reaction, a chemical system showing similar patterns. We verified the linear relationship between the normal velocity and the curvature of wave fronts predicted by a reaction–diffusion model. The proportionality factor, which in this case is the diffusion coefficient of the chemical signal transmitter cAMP establishing communication between the cells, was determined to be $0.66\times10^{-5}\,cm^2s^{-1}$. From measurements of positively curved circular waves, we could roughly estimate the critical radius of wave propagation R_{crit} ($\sim200\,\mu m$); which means that up to 500 cells are necessary to form a center of an aggregation structure. Furthermore, we analyzed the geometrical parameters of spiral wave patterns and estimated the core radius r_0 to be $\approx300\,\mu m$.

Key words: *Dictyostelium discoideum*, aggregation pattern, computerized image processing, spiral wave patterns.

Introduction

The slime mould, *Dictyostelium discoideum*, which shows waves of aggregation movement during the early stage of its development cycle, is an important biological model system for the analysis of pattern formation during morphogenetic development (Gerisch, 1971). The aggregation patterns forming in this living excitable system are similar to the patterns found in the chemical Belousov–Zhabotinskii reaction with geometries such as expanding concentric circles or rotating spirals. This phenomenological similarity is reflected on a mathematical level by the fact that the models describing these two systems both belong to a general class of coupled reaction–diffusion equations. Kęener and Tyson (1986) have developed a general theoretical approach to the description of waves in excitable systems, which they apply to spatial patterns in the *Dictyostelium* system by extending a model of Martiel and Goldbeter.

In this paper, we first give a short introduction to the biological background and describe the model and the experimental methods. We then present results obtained by computerized analysis of the patterns detected by a dark-field equipment combined with video techniques. Quantitative data are provided in terms of wave velocity and geometry that prove the theoretically predicted linearity between the normal propagation velocity and the curvature of wave fronts (Keener and Tyson, 1986). Furthermore, we analyze the detected spiral structures and discuss their geometrical shape as well as the properties of the spiral core.

Materials and methods

(1) The System

When the food source of *Dictyostelium discoideum* cells is exhausted, their development cycle is initiated. The first step in this cycle is the aggregation phase during which the amoebae aggregate into clusters of about 10^5 cells. The aggregation movement arises from chemical waves of cyclic adenosine 3′,5′-monophosphate (cAMP) traveling through the cell population, by which the cells communicate among each other (Loomis, 1975, 1982). 4 to 6 h after the beginning of starvation some cells (center cells) start to produce cAMP in a periodical manner. This cAMP is secreted into the extracellular medium and binds to a cAMP-specific membrane receptor located at the surface of the neighbouring cells. The binding stimulates the synthesis of cAMP inside the cell (Devreotes *et al.* 1979). In this way, the signal is conducted and amplified. After such a stimulus of cAMP the receptor becomes desensitized (Devreotes and Sherring, 1985; Newell, 1982) for a certain period of time. This refactory period guarantees that cAMP waves can travel only outwards. Behind each wave, the cAMP is reduced by extracellular and membrane-bound phosphodiesterases.

While the waves pass periodically through the field of cells, a secondary response of the cells is a chemotactic movement towards the center of the pattern, where they form a multicellular slug. In a final step, the slug develops into a fruiting

body, carrying the spores with which the development cycle can start again.

(2) The Martiel–Goldbeter model

The cAMP signaling system is described in a model developed by Martiel and Goldbeter (1987), which accounts for the processes: secretion of cAMP by the cells, hydrolysis of cAMP by phosphodiesterase, binding of the secreted cAMP to the membrane receptor with a resulting stimulation of cAMP production, and desensitization of the membrane receptor. The main components of this model are cAMP and the receptor, which can exist in a sensitized and desensitized state (Devreotes and Sherring, 1985; Vaughan and Devreotes, 1988) and thus allows the description of active and passive phases of the cAMP synthesis.

The model leads to a system of three coupled nonlinear ordinary differential equations describing the dynamic interaction of the intracellular cAMP (β), the extracellular cAMP (γ) and the fraction of active membrane receptors (ρ). With appropriately chosen parameter sets for the rate constants, Martiel and Goldbeter (1987) were able to model both oscillations and relay of cAMP signals, in agreement with experimental investigations.

(3) Cyclic AMP waves

In order to model cAMP waves in monolayered cultures of *Dictyostelium* cells on agar surfaces, where the secreted cAMP diffuses through the aqueous extracellular medium, the Martiel-Goldbeter model has to be supplemented by terms describing the diffusion of the extracellular cAMP (γ).

Tyson *et al.* proposed a reduced system of two reaction–diffusion equations for γ and ρ which can be written in the following form (Tyson *et al.* 1989; Tyson and Murray, 1989):

$$\frac{\partial \gamma}{\partial t} = \epsilon \Delta \gamma + \frac{1}{\epsilon}[s\phi(\rho,\gamma) - \gamma]$$
$$\frac{\partial \rho}{\partial t} = -f_1(\gamma)\rho + f_2(\gamma)(1-\rho), \quad (1)$$

where ϵ is a scaling parameter, s, ϕ, f_1 and f_2 are specified in Tyson *et al.* (1989), Δ is the Laplacian operator describing the diffusion of the variable γ.

From this type of equation a linear relationship between the propagation velocity and the curvature of travelling cAMP waves can be derived (see Appendix):

$$N = c - D \cdot K. \quad (2)$$

N is the normal velocity, c the velocity of plane waves, D the diffusion coefficient of the autocatalytic species cAMP, and K is the curvature of the waves.

The main statements of Equation (2) are: (1) for negative curvature the normal velocity increases with increasing curvature; (2) for positive curvature, it decreases with increasing curvature; (3) there exists a minimal radius below which propagation of circular waves will not take place.

Furthermore, Equation 1 has, under quite general conditions, periodic wave solutions that satisfy a dispersion relation (Tyson and Keener, 1988; Foerster *et al.* 1988; Dockery *et al.* 1988).

$$c = \sigma(T). \quad (3)$$

This relationship expresses the dependence of the propagation velocity (c) on the temporal period of the wave train (T). It shows an increase in the velocity of wave propagation with increasing period of wave initiation T, reaching an asymptotic value c_{max} as $T \to \infty$. Below a minimal value of T, no wave trains can exist because the membrane receptor cannot become sensitive again between the successive wave trains. It should be added that σ is a complex function of the reaction kinetics and the scaling parameter ϵ.

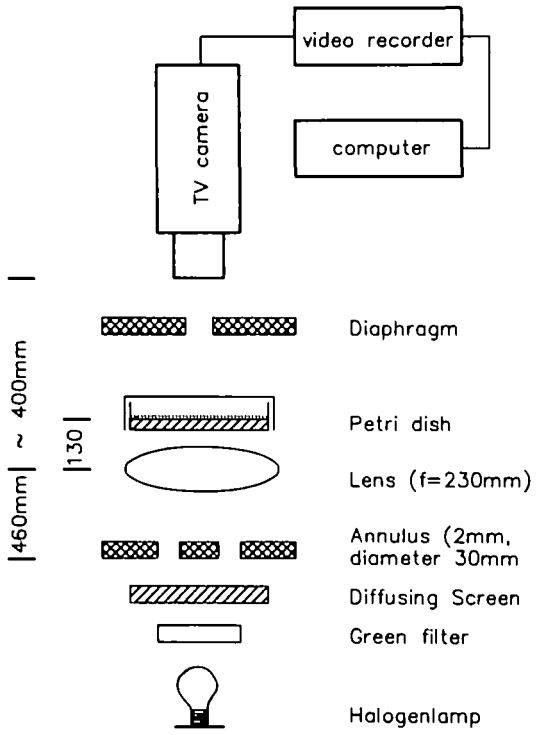

Fig. 1. Schematic diagram of the dark-field equipment.

(4) Experimental methods

The cells of *Dictyostelium discoideum*, axenic strain AX-2, were cultivated on nutrient medium and harvested at a density of 5×10^6 cells ml^{-1}, washed three times with buffer and spread on an agar surface in a Petri dish at a density of 4×10^5 cells cm^{-2}. The dishes were stored in the dark at 21 °C for 4–6 h.

The cells respond to the cAMP waves by travelling in the direction opposite to the cAMP wave propagation. The moving cells have an elongated shape in contrast to the resting circular cells. Because of the different scattering behaviour of the elongated (moving) and the circular (resting) cells the moving bands appear in our dark-field optics (Gross *et al.* 1976) (Fig. 1) as bright stripes whereas the resting bands appear as dark stripes. We recorded movies at 40 ms intervals with a video camera (Hamamatsu C1000) on a Umatic video recorder (Sony).

In order to verify Equation 2 experimentally for negative curvature, we measured the temporal evolution of cusp-like structures formed after the collision of waves using video imaging techniques (Müller *et al.* 1985). Computerized evaluation procedures combined with pseudocolour techniques were applied to extract a set of single isointensity data points along the edge of the cusplike structure, i.e. along the narrow line separating the bright and dark stripes. These data sets were fitted by hyperbolas (Fig. 2) and the curvatures were determined in the vertices (Foerster *et al.* 1988). The velocity of the waves was measured with help of a timer that marked each video picture.

For the analysis of the velocity–curvature relationship for positive curvature, we followed the evolution of circular waves. Since these are rare events, only a very limited amount of data was available. We determined the radius of the

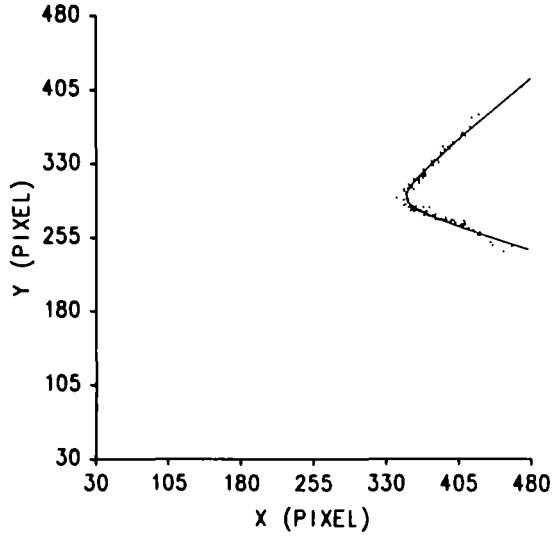

Fig. 2. Hyperbolic fit to data points of the cusp structure formed by colliding bands. Pixel resolution: ≈37 μm per pixel.

circular wave as a function of time, after selecting isointensity data points at the edge of the circular structure (Foerster *et al.* 1989). The resulting data points were fitted by a third order polynomial. From this fit, the velocity was derived as a function of the wave radius or its curvature.

Spiral patterns were analyzed by extracting contour maps from single contour data with the same technique as described above, as well as from contour maps obtained from the whole set of data by choosing all the isointensity data points obtained along the dark/bright stripes at the edge of the spiral structure (Foerster *et al.* 1988). These contours were followed up to their innermost end point, where they merge into a small dark spot. Successive spiral contours were then overlaid to determine parameters such as period length and radius of the spiral core. For this purpose, the full contour data sets were fitted by polygons of appropriate order.

Results

Fig. 2 shows an example for a data set extracted for one of the two cusps formed in the area of wave collision (see also Fig. 5A–D). The data points are overlapped with the fitted hyperbola. The relation between the normal velocity and the curvature of the fronts, as determined from a sequence of hyperbola fitted to a series of successive video pictures, is shown in Fig. 3. The propagation velocity of the plane wave (zero curvature) was determined from the outward motion of very large circular waves, yielding 5.6 $\mu m\,s^{-1}$ (compare the value of 4.2 $\mu m\,s^{-1}$ reported in Alcantara and Monk (1974)).

The slope of the regression line drawn in this figure is $0.66\pm0.05\times10^{-5}\,cm^2s^{-1}$. According to Equation 2, it corresponds to the diffusion coefficient D of cAMP. In Dworkin and Keller (1977), this diffusion coefficient was determined to be $0.4\times10^{-5}\,cm^2s^{-1}$. By analysing diffusion profiles of NADH in an agar layer, detected at 340 nm, we obtained for its diffusion coefficient a value of $0.47\times10^{-5}\,cm^2s^{-1}$. (NADH was chosen because its size is comparable to that of cAMP).

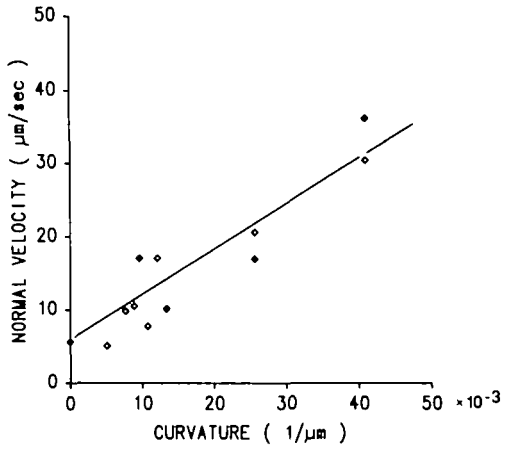

Fig. 3. Relation between negative curvature and normal velocity determined from cusp structures as shown in Fig. 2. The slope of the regression line is $0.66\pm0.05\times10^{-5}\,cm^2s^{-1}$. It intercepts with the velocity axis at 5.6 $\mu m\,s^{-1}$.

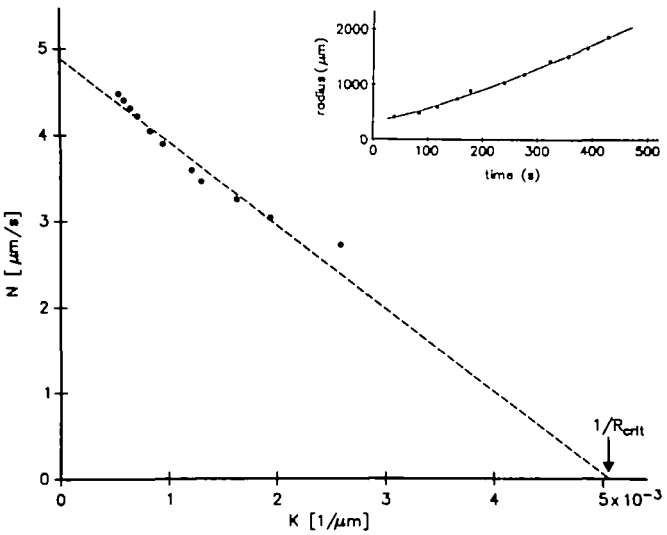

Fig. 4. Relation between positive curvature and normal velocity determined from the radius of an outward propagating circular wave shown in the inset. The slope of the regression line is $0.93\pm0.06\times10^{-5}\,cm^2s^{-1}$, the intercept with the velocity axis is 4.8 $\mu m\,s^{-1}$. The intercept with the curvature axis yields a critical radius $R_{crit}\approx200\,\mu m$.

In Fig. 4, the relation between normal velocity and positive curvature is presented, as obtained from a polynomial fit to the growing radius of an outward propagating circular wave shown in the inset of the figure. The velocity-curvature data determined from the polynomial fit are fitted by a regression line drawn with a slope of $0.93\pm0.06\times10^{-5}\,cm^2s^{-1}$. By extrapolation of this line to the intersects with the velocity and the curvature axis, one gets estimates for the plane wave velocity, $c=4.88\,\mu m\,s^{-1}$, and the critical radius, $R_{crit}\approx200\,\mu m$.

Fig. 5 A–D shows a sequence of original spiral patterns detected in the dark-field optics at time inter-

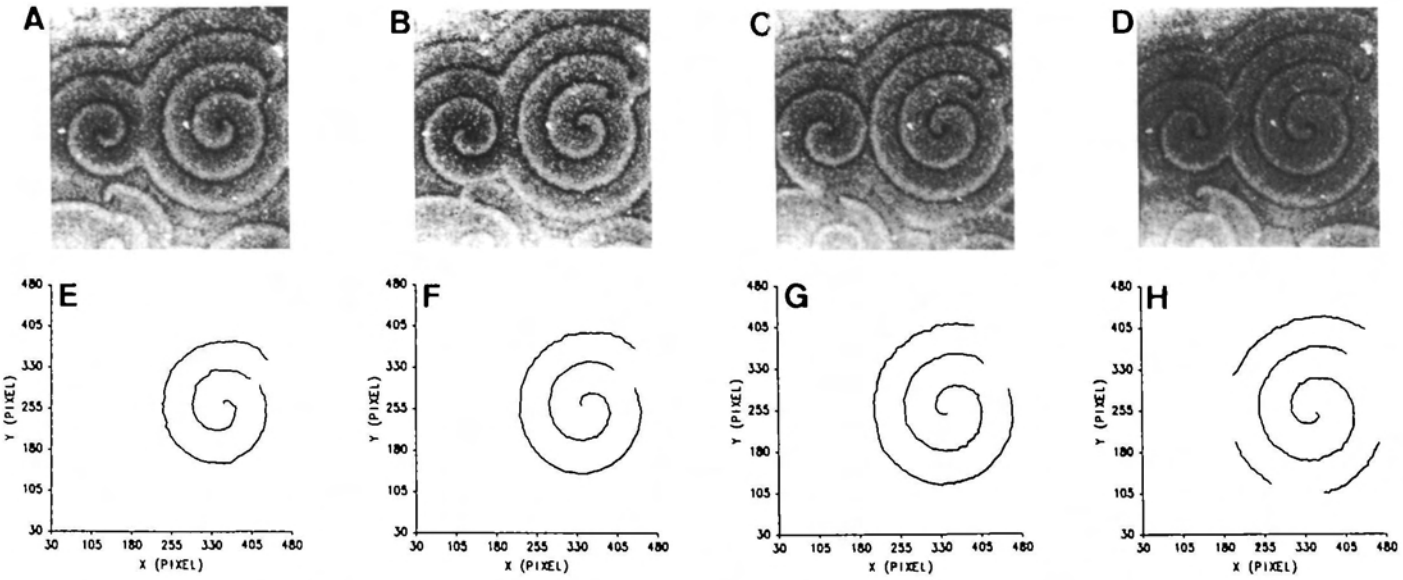

Fig. 5. (A–D) Sequence of original dark-field spiral patterns; picture area: $1.9 \times 1.9\,cm^2$, time interval between successive pictures: ≈120 s. (E–H) Contour maps extracted from the corresponding pictures (A–D).

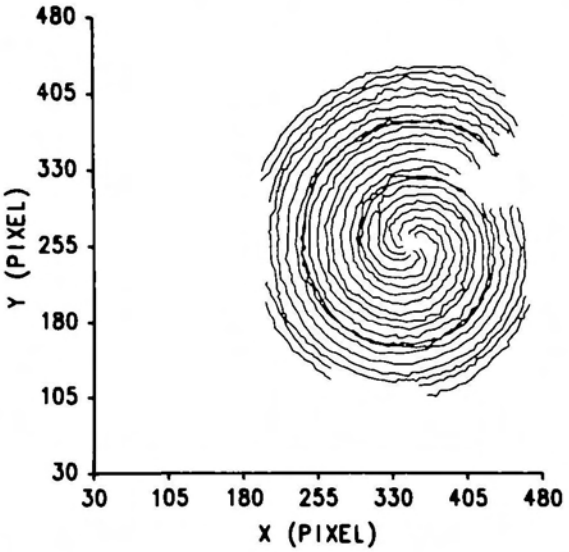

Fig. 6. Overlay of eight spiral contours such as shown in Fig. 5E–H. Time interval between successive contour maps ≈60 s; radius of the core region $r_o \approx 300\,\mu m$.

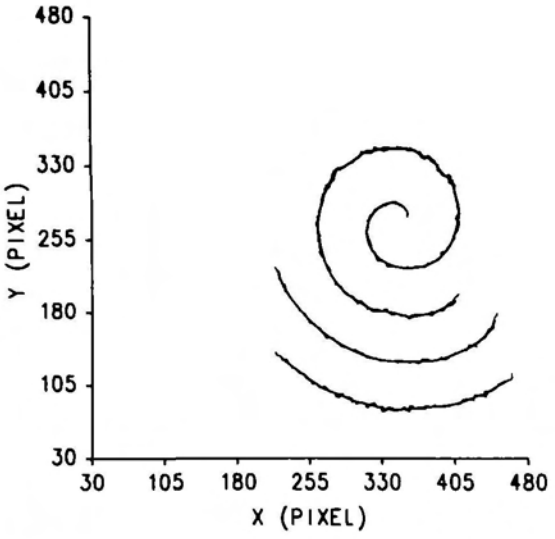

Fig. 7. Whole data set of an isointensity level at the edge of a spiral overlapped with a spline fit.

vals of 120 s between the successive pictures. This sequence also illustrates the annihilation process of colliding waves and the evolution of the cusp-like structures. In Fig. 5E–H contour maps are drawn. These were extracted along the outer edge of the spiral structure obtained from the corresponding pictures after reducing noise by applying a 3×3 pixel moving average.

An overlay of such spiral contours is presented in Fig. 6. The overlay consists of eight contour maps taken at 60 s intervals, including those of Fig. 5E–H, and visualizes the size of the spiral core, at the boundary of which the contour maps end. This is the region around which the spiral rotates and which remains in a stable stationary state during rotating, and which is identical with the dark spot. Its radius r_o is $\approx 300\,\mu m$.

In Fig. 7 the spiral pattern, obtained by taking the whole set of contour data, is overlapped with a spline fit. From the spline fit data the pitch of the spiral was determined as a function of the bow length. It is nearly constant (2 mm) except for the core region where the pitch is slightly larger (≈2.2 mm). The velocity of the outward propagating structure is $4.6\,\mu m\,s^{-1}$, which results in a rotation period of 430–480 s (7–8 min). This is in good agreement with other experiments ($5\,\mu m\,s^{-1}$ and 7 min, respectively in Tomchik and Devreotes (1981)) and with the estimates obtained from the reaction–diffusion equation (A1) ($4\,\mu m\,s^{-1}$ and 7.5 min (Tyson and Keener, 1988).

Discussion and Conclusion

The observed linearity between normal velocity and negative curvature (Fig. 3) is expressed in a proportionality factor, which is in good agreement with the expected diffusion coefficient for cAMP. This is a further experimental proof for the validity of the 'curvature' equation for excitable media (Equation 2) as already established for waves in the BZ system (Foerster *et al.* 1988). It emphasizes the general validity of the mechanism of diffusion-controlled propagation of waves in excitable media. Although our estimates for positively curved waves are only preliminary, they also support the predicted curvature relationship. The diffusion coefficient D, as well as the extrapolated plane wave velocity c, found by both methods are in the same order of magnitude. Using the values for D and c determined from negatively curved waves, the minimum radius of the pacemaker necessary to initiate waves, $R_{crit}=D/c$, is estimated to be $\approx 130\,\mu m$. Thus, it is smaller than the extrapolated value $R_{crit}\approx 200\,\mu m$ obtained from Fig. 4, but in view of the small number of data available for positive curvature, this can be considered as a good agreement. With a cell density of 4×10^5 cells cm^{-2} $R_{crit}\approx 130$ and $\approx 200\,\mu m$, respectively, means that the pacemaker area should contain $\approx$200–500 cells that have to oscillate synchronously to initiate circular patterns of aggregation waves.

It should be mentioned that there exists an alternative theory, developed by Zykov and Morozova (1979), which predicts a critical radius that corresponds to a finite velocity value. Our limited amount of data for positively curved waves does not permit to verify this prediction. However, the extrapolated critical radius can be taken as the minimum radius for the wave propagation.

The influence of curvature on the propagation velocity of chemical waves becomes significantly important only for high values, positive or negative, as in the case of very small target patterns, spiral structures near the core, and highly negatively curved areas of colliding waves. For concentric circular waves far from the origin the wave fronts are nearly planar, so that curvature becomes vanishingly small and the structures have to obey only the dispersion relation. For this reason, target patterns can exist with various periods, but each pattern propagation with a velocity defined by the dispersion relation $c=\sigma(T)$ (see Experimental methods). It describes the characteristic decrease of wave velocity when the time between two successive wave trains decreases, so that the *Dictyostelium* cells have less time to recover excitability. This accounts for the fact that the cAMP-specific membrane receptor needs a certain period of time to recover full sensitivity. The dispersion relation for the used AX-2 strain was measured by Siegert *et al.* (Siegert and Weijer, 1989).

In spiral waves, curvature is not negligible in the core region and therefore they must satisfy both the curvature-velocity relationship and the dispersion relation. Consequently, spiral waves have characteristic c,T values which satisfy both conditions. These values are functions of the size of the spiral core. From a numerically computed spiral wave Tyson and Keener (1988) calculated a core radius $r_o\approx 200\,\mu m$; the value measured by overlaying successive contour maps is $r_o\approx 300\,\mu m$. This extended core region containing a high amount of core cells supports the suggestion of Durston (1973), that the core, the region around which the spiral is rotating, is built by a loop of cells around which a continuous circulation of an excitation wave takes place.

Furthermore, our observation that the pitch as a function of the bow length is nearly constant except for the core region, as well as the detection of an extended core region on the basis of the overlay picture in Fig. 6 suggest that the spiral pattern of *Dictyostelium discoideum* resembles more an involute of a circle than an Archimedean spiral.

In conclusion, our results provide quantitative evidence that the mechanism of the cAMP-signal-relaying system underlies the general conditions of excitable media. They strongly support the concept that the theoretical investigations of excitable media, as mainly done for simpler systems, e.g. the chemical Belousov–Zhabotinskii reaction, allow predictions for systems of higher complexity like the *Dictyostelium discoideum* cell population. This should lead to a better understanding of such complex processes as morphogenetic development.

We thank Professor G. Gerisch, F. Siegert and Dr K. Weijer for advice in microbiological preparations and their hospitality, Professor G. Gerisch also for generously supplying AX-2 spores, Dr Th. Plesser for computational help, V. Zimmermann and K.-H. Müller for software programming, G. Rudek and A. Rietig for laboratory assistance. This work was supported by the Stiftung Volkswagenwerk, Hannover.

Appendix

The equation system (1) belongs to a more general class of models describing wave propagation in excitable media, e.g. chemical waves in the Belousov–Zhabotinskii reaction (Keener and Tyson, 1986; Tyson and Keener, 1988):

$$\epsilon\frac{\partial u}{\partial t} = \epsilon^2\triangle u + f(u,v)$$
$$\frac{\partial v}{\partial t} = \epsilon\triangle v + g(u,v), \qquad \text{(A1)}$$

where u and v are the system variables, f(u,v)) and g(u,v) are nonlinear functions describing the reaction kinetics, and $\triangle$ is the Laplacian operator describing the diffusion of the variables. From this type of equation system, equation (2) (the so-called 'eikonal' equation) regarding the temporal and spatial development of the travelling wave geometry is derived (Keener and Tyson,

1986; Keener, 1986; Foerster *et al.* 1988), which is in explicit form:

$$\frac{\frac{\partial y}{\partial t}}{\left(1+\left(\frac{\partial y}{\partial x}\right)^2\right)^{1/2}} = c - D\cdot\frac{\frac{\partial^2 y}{\partial x^2}}{\left(1+\left(\frac{\partial y}{\partial x}\right)^2\right)^{3/2}}. \quad \text{(A2)}$$

References

Alcantara, F. and Monk, M. (1974). Signal propagation during aggregation in the slime mould *Dictyostelium discoideum*. *J. gen. Microbiol.* **85**, 321–324.

Devreotes, P. N., Derstine, P. L. and Steck, T. L. (1979). Cyclic 3′,5′ AMP relay in Dictyostelium discoideum. I. A technique to monitor responses to controlled stimuli. *J. Cell Biol.* **80**, 291–299.

Devreotes, P. N. and Sherring, J. A. (1985). Kinetics and concentration dependence of reversible cAMP induced modification of the surface cAMP receptor in Dictyostelium. *J. biol. Chem.* **260**, 6378–6384.

Dockery, J. D., Keener, J. P. and Tyson, J. J. (1988). Dispersion of traveling waves in the Belousov-Zhabotinskii reaction. *Physica* **D30**, 177–191.

Durston, A. J. (1973). Dictyostelium discoideum aggregation fields as excitable media. *J. theor. Biol.* **42**, 483–504.

Dworkin, M. and Keller, K. H. (1977). Solubility and diffusion coefficient of adenosine 3′:5′ monophosphate. *J. biol. Chem.* **252**, 864–865.

Foerster, P., Müller, S. C. and Hess, B. (1988). Curvature and propagation velocity of chemical waves. *Science* **241**, 685–687.

Foerster, P., Müller, S. C. and Hess, B. (1989). Critical size and curvature of wave formation in an excitable chemical medium. *Proc. natn. Acad. Sci. U.S.A.* **86**, 6831–6834.

Gerisch, G. (1971). Periodische Signale steuern die Musterbildung in Zellverbänden. *Naturwissenschaften* **58**, 430–438.

Gross, J. D., Peacey, M. J. and Trevan, D. J. (1976). Signal emission and signal propagation during early aggregation in Dictyostelium discoideum. *J. Cell. Sci.* **22**, 645–656.

Keener, J. P. (1986). A geometrical theory for spiral waves in excitable media. *SIAM J. Appl. Math.* **46**, 1039–1056.

Keener, J. P. and Tyson, J. J. (1986). Spiral waves in the Belousov-Zhabotinskii reaction. *Physica* **21D**, 307–324.

Loomis, W. F. (1975). Dictyostelium discoideum. *A Developmental System*. New York: Academic Press.

Loomis, W. F. (1982). *Development of Dictyostelium*, San Diego, CA: Academic Press.

Martiel, J.-L. and Goldbeter, A. (1987). A model based on receptor desensitization for cyclic AMP signalling in Dictyostelium cells. *Biophys. J.* **52**, 807–828.

Müller, S. C., Plesser, Th. and Hess, B. (1985). Two-dimensional spectrophotometry with high spatial and temporal resolution by digital video techniques and powerful computers. *Anal. Biochem.* **146**, 125–133.

Newell, P. C. (1982). Cell surface binding of adenosine to Dictyostelium and inhibition of pulsatile signalling. *FEMS Microbiology Letters* **13**, 417–421.

Siegert, F. and Weijer, C. (1989). Digital image processing of optical density wave propagation in *Dictyostelium discoideum* and analysis of the effects of caffeine and ammonia. *J. Cell Sci.* **93**, 315–335.

Tomchik, K. J. and Devreotes, P. N. (1981). Adenosine 3′,5′-monophosphate waves in *Dictyostelium discoideum*: a demonstration by isotope dilution-fluorography. *Science* **212**, 443–446.

Tyson, J. J., Alexander, K. A., Manoranjan, V. S. and Murray, J. D. (1989). Spiral waves of cyclic AMP in a model of slime mould aggregation. *Physica* **D34**, 193–207.

Tyson, J. J. and Keener, J. P. (1988). Singular perturbation theory of traveling waves in excitable media (A review). *Physica* **D32**, 327–361.

Tyson, J. J. and Murray, J. D. (1989). Cyclic AMP waves during aggegation of Dictyostelium amoebae. *Development* **106**, 421–426.

Vaughan, R. A. and Devreotes, P. N. (1988). Ligand-induced phosphorylation of the cAMP receptor from Dictyostelium discoideum. *J. biol. Chem.* **263**, 14 538–14 543.

Zykov, V. S. and Morozova, O. L. (1979). Speed of spread of excitation in a two-dimensional excitable medium, *Biophysics* **24**, 739–744.

(*Accepted 7 February 1990*)